Cellular models for fundamental and applied biomedical research

Liu, J.

Chapter 5

Generation of conditionally immortalized brown pre-adipocytes with preserved adipogenic capacity

Jia Liu, Sander Kooijman, Eline N. Kuipers, Hetty C. M. Sips, Patrick C. N. Rensen, Martin J. Schalij, Daniël A. Pijnappels,Antoine A.F. de Vries

To be submit

Abstract

Brown adipose tissue (BAT) is regarded as a potential target to treat obesity and associated metabolic disorders because of its capacity to take up and combust glucose and fatty acids for thermoregulation. However, its cellular and molecular investigation has been hampered due to high cellular heterogeneity and a limited availability of cell material. In this study, monoclonal lines of conditionally immortalized brown preadipocytes (iBPAs) were generated, using mouse BAT as starting material. These cell lines retain long-term proliferation as well as adipogenic capacity. RT-qPCR analyses showed that brown fat markers including uncoupling protein 1 (Ucp1) were highly expressed in brown fat cells differentiated from iBPAs. Furthermore, the differentiated cells responded to β3-adrenergic stimulation by increasing glycerol release and *Ucp1* expression. iBPA-derived brown fat cells may represent an easy-to-use model system for fundamental and applied research into BAT.

Introduction

Obesity results from energy intake exceeding expenditure and is a major risk factor for metabolic disorders. A positive energy balance leads to storage of excess energy mainly in adipose tissue[1,2]. In mammals, two major types of functionally distinct adipose tissue exist, *i.e.* white adipose tissue (WAT) and brown adipose tissue (BAT)[3]. WAT is specialized in storing energy in the form of triglycerides[4-6], while brown adipocytes dissipate energy for heat production by uncoupling the electron transport chain from ATP synthesis through expression of uncoupling protein 1 (UCP1)[4,7-11]. As a result, BAT represents a therapeutic target to enhance energy expenditure and combat obesity and related metabolic disorders[2,12,13].

The development of therapeutic strategies based on BAT is hampered by the lack of proper brown adipocyte cell culture models. As mature adipocytes are post-mitotic and thus unable to multiply themselves *in vitro*, the formation of sufficient brown adipocytes for experiments requires proliferation and differentiation of adipocyte precursors. Over the last years, a number of different murine brown preadipocyte (BPA) lines have been generated such as BFC-1[14], HB2[15], HIB 1B[16,17] and T37i[18]. Although these cell lines have been helpful in increasing the understanding of adipocyte biology, they all possess some inherent disadvantages limiting their usefulness as model systems to study the properties of brown fat. BCF-1 cells are spontaneously immortalized cells derived from interscapular BAT but do not express detectable amounts of *Ucp1* following differentiation even after adrenergic stimulation with isoproterenol[19]. HB2 cells are brown preadipocytes isolated from the interscapular BAT of p53 knockout mice, while HIB 1B and T37i cells were derived from transgenic mice expressing the simian virus 40 (SV40) large T (LT) antigen using constitutively active, lineage-restricted promoters to drive transgene expression. While these transgenic cells all express *Ucp1* following adipogenic differentiation and proper stimulation, their gene expression profiles may not accurately recapitulate that of native brown fat cells as both p53 and LT have been shown to affect formation of brown adipocytes[20,21]. Moreover, continuous proliferation pressure due to permanent immortalization may alter the differentiation capacity of BPAs causing their differentiated progeny to functionally differ from primary brown fat cells. Indeed, HB2 cells display a passage number-dependent decrease in the ability to express *Ucp1* following adipogenic differentiation and adrenergic stimulation[15]. These drawbacks prompted us to generate conditionally immortalized monoclonal BPA (iBPA) lines of mice by using a lentiviral vector (LV) expressing LT in a doxycycline (dox)/tetracycline-dependent manner to control cell proliferation[22]. The resulting monoclonal cell lines were characterized in terms of their dox-dependent LT expression level and proliferation capacity and their ability to undergo adipogenic differentiation in the presence of insulin and rosiglitazone using multilocular lipid droplet formation and expression of brown fat marker genes as read-out systems. Finally, the effects of adrenergic stimulation on the glycerol secretion and *Ucp1* mRNA expression of adipogenically differentiated iBPAs was studied.

Materials and Methods

Construction of plasmids

DNA constructions were carried out with enzymes from Fermentas (Thermo Fisher Scientific, Breda, the Netherlands) or from New England Biolabs (Bioke´, Leiden, the Netherlands) and with oligodeoxyribonucleotides from Sigma-Aldrich (Zwijndrecht, the Netherlands) using established procedures or following the instructions provided with specific reagents.

Plasmid pAT153.SV40ori(-)*ts*A58, which codes for the temperature-sensitive mutant of the oncogenic SV40 LT antigen designated *ts*A58[23], was used as template in a polymerase chain reaction (PCR) with VELOCITY DNA polymerase (GC Biotech, Alphen aan den Rijn, the Netherlands) and primers 5' AAGGATCCGTGCACCATGGATAAAGTTTTAAACAGAGAGGA 3' and 5' CCGAATTCTTTATGTTTCAGGTTCAGGG 3' (the LT initiation codon and the complement of its termination codon are underlined). The resulting PCR fragment was inserted into plasmid pJET1.2/blunt using the CloneJET PCR cloning kit (Thermo Fisher Scientific) to generate pJet1.2.LT-*ts*A58. pJet1.2.LT-*ts*A58 was incubated with BamHI and EcoRI and the 2.5-kb digestion product was combined with the 11.5-kb BamHI×EcoRI fragment of SIN-LV shuttle plasmid pLVET.tTS.dEcoRI to generate pLV.ihEEF1A1.LT-*ts*A58. pLVET.tTS.dEcoRI is a derivative of pLVET-tTR-KRAB[22] (Addgene, Cambridge, MA; plasmid number: 116444). It was made by digestion of pLVET-tTR-KRAB with EcoRI and NheI and ligation of the resulting 1.6-kb fragment encoding the encephalomyocarditis virus internal ribosomal entry site and the tetracycline-controlled transrepressor protein TetR-KRAB[24] to the 10.8-kb EcoRI×BcuI fragment of pLVET-tTR-KRAB.

LV production

LV production was carried out as detailed before[25]. To generate vesicular stomatitis virus G protein-pseudotyped particles of LV.ihEEF1A1.LT-*ts*A58, subconfluent monolayers of 293T cells were transfected with LV shuttle construct pLV.ihEEF1A1.LT-*ts*A58 and the packaging plasmids psPAX2 (Addgene; plasmid number: 12260) and pLP/VSVG (Thermo Fisher Scientific) at a molar ratio of 2:1:1. The 293T cells were cultured in high-glucose Dulbecco's modified Eagle's medium (DMEM; Life Technologies Europe, Bleiswijk, the Netherlands; catalogue number: 41966) with 10% fetal bovine serum (FBS; Life Technologies Europe). The transfection mixture consisted of 35 µg of plasmid DNA and 105 µg of polyethyleneimine (Polysciences Europe, Eppelheim, Germany) in 2 ml of 150 mM NaCl per 175-cm^2 cell culture flask (Greiner Bio-One, Alphen aan den Rijn, the Netherlands) and was directly added to the culture medium. The next morning, the transfection medium was replaced by 15 ml of fresh high-glucose DMEM supplemented with 5% FBS and 25 mM HEPES-NaOH (pH 7.4). At ± 48 hours after the addition of plasmid DNA to the producer cells , the culture supernatants were harvested and cleared from cellular debris by centrifugation at room temperature (RT) for 10 min at 3,750×*g* and subsequent filtration through 0.45-µm pore-sized, 33-mm diameter polyethersulfone Millex-HP syringe filters (Millipore, Amsterdam, the Netherlands). To concentrate and purify the LV particles, 30 ml of vector suspension

in a 38.5-ml polypropylene ultracentrifuge tube (Beckman Coulter Nederland, Woerden, the Netherlands) was underlayed with 5 ml of 20% (wt/vol) sucrose in phosphate-buffered saline (PBS) and spun for 120 min at 4°C with slow acceleration and without braking at 15,000 revolutions per min in an SW32 rotor (Beckman Coulter Nederland). Next, the supernatants were removed and the pellets were suspended in PBS-1% bovine serum albumin (BSA; Sigma-Aldrich, St. Louis, MO) by overnight incubation with gentle shaking at 4°C. The concentrated vector suspension was divided on ice in 50 µl aliquots for storage at -80°C.

Isolation and culture of primary murine BPAs

Primary murine BPAs were isolated from the interscapular BAT depot of 4-week-old male C57Bl/6J mice (Charles River Laboratories International, Wilmington, MA). Isolated tissue was minced with scissor into 3- to 4-mm pieces, washed once with DMEM/F-12 GlutaMAX (Thermo Fisher Scientific; catalogue number: 10565018) and incubated in DMEM/F-12 GlutaMAX containing 1 mg/mL collagenase type I (Thermo Fisher Scientific; catalog number: 17018029) at 37°C for 45 min. After centrifugation and resuspension in growth medium (DMEM/F-12 GlutaMAX supplemented with 10% heat-inactivated FBS, 100 U/mL penicillin and 100 µg/mL streptomycin), cells were filtered through a 200-µm pore-sized nylon filter (Sefar, Lochem, the Netherlands; catalogue number: 03-200/39) and seeded into a culture flask. Growth medium was replaced the following day and then every other day.

Transduction of primary murine BPAs and generation of lines of conditionally immortalized mouse BPAs

At passage two, *i.e.* after approximately 8 population doublings (PDs), the primary murine BPAs were transduced with LV.ihEEF1a1.SV40-LT-*ts*A58. The next day, the inoculum was replaced by growth medium containing 100 ng/ml dox (Sigma-Aldrich) to induce LT expression. The cells were subsequently given fresh growth medium with dox every other day. After 1 week of culture, the transduced cells were trypsinized and plated at a low density of 10~20 cells/cm^2 to allow formation of single-cell clones. Two to 3 weeks later, individual cell colonies were picked and separately expanded in the presence of dox.

Culture, differentiation and adrenergic stimulation of murine iBPAs

Murine BPA clones were cultured in growth medium supplemented with 100 ng/mL dox. Growth medium was replaced every other day and cells were split 1:8 after reaching approximately 70% confluency. For differentiation, cells were allowed to grow confluent and 2 days later exposed to growth medium containing 5.6 nM bovine insulin (Sigma-Aldrich; catalogue number: I0305000), 25 µg/mL sodium ascorbate (Sigma-Aldrich; catalogue number: A-7631) and 1 µM of the peroxisome proliferator-activated receptor γ agonist rosiglitazone (Sigma-Aldrich; catalogue number: R2408), 10 mM HEPES (adjusted to pH 7.40 with NaOH). This so-called adipogenic differentiation medium was replaced every other day and the various clones were screened for their adipogenic capacity, *i.e.* their ability to develop multilocular lipid droplets and to express the brown fat marker gene *Ucp1*. Next, differentiated BPAs were stimulated with 1 µM of the broad-spectrum adrenoreceptor agonist noradrenalin

(NA), 10 μM of the highly selective β3 adrenoreceptor agonist CL316243 or vehicle (PBS) for 8 hours. Subsequently, supernatant was collected for colorimetric determination of glycerol production (INstruchemie, Delfzijl, the Netherlands) and cells were lysed in TriPure (Roche Life Science, Almere, the Netherlands) for RNA and protein analysis as described below.

Analysis of cell proliferation

To draw growth curves, the primary murine BPAs and conditionally immortalized cells were subcultured 1:4 and 1:8 on reaching confluency so that each passage corresponded to 2 and 3 PDs, respectively. To assess their proliferation rate and dependence on the activity of SV40 LT antigen, the murine iBPAs were cultured at low density in medium with or without 100 ng/ml dox. At different days after culture initiation, cells were collected in medium and counted using an Accuri flow cytometer (BD Biosciences, Breda, the Netherlands).

Western blotting

Western blotting was carried out as detailed before[26]. After blocking, the membranes were incubated overnight at 4°C with primary mouse monoclonal antibodies directed against LT (1:2,000; Santa Cruz Biotechnology, Dallas, TX; catalogue number: sc-147) or glyceraldehyde 3-phosphate dehydrogenase (GAPDH; loading control; 1:100,000; Millipore; catalogue number: MAB374) and then probed with goat anti-mouse IgG secondary antibodies linked to horseradish peroxidase (1:15,000; Santa Cruz Biotechnology) for 1 hour at RT. Chemiluminescence was produced using the SuperSignal West Femto maximum sensitivity substrate (Thermo Fisher Scientific), captured by a ChemiDoc XRS imaging system (Bio-Rad Laboratories, Veenendaal, the Netherlands) and analysed by Quantity One software (Bio-Rad Laboratories) using the GAPDH signals for normalization purposes.

Immunocytology

Cells were processed for immunostaining as previously described[27]. Detection of LT was done with the same primary antibody as used for the analysis of LT expression by western blotting. Actively replicating were detected using polyclonal rabbit anti-Ki-67 antibodies (Abcam, Cambridge, United Kingdom; catalogue number: ab15580), The primary antibodies were diluted 1:200 in PBS containing 0.1% normal donkey serum (Sigma-Aldrich) and left on the cells overnight at 4°C. Bound antigens were detected using Alexa 488-conjugated donkey anti-rabbit IgG (H+L) (Thermo Fisher Scientific; catalogue number: A21206) and Alexa 568-coupled donkey anti-mouse IgG (H+L) (Thermo Fisher Scientific; catalogue number: A10037). These secondary antibodies were diluted 1:400 in PBS. Hoechst 33342 (10 μg/μl; Thermo Fisher Scientific) was used to counterstain nuclei. Stained cells were visualized using a digital color camera-equipped fluorescence microscope (Nikon Eclipse 80i; Nikon Instruments Europe, Amstelveen, the Netherlands).

RNA isolation, cDNA synthesis and reverse transcription-quantitative PCR (RT-qPCR) analysis

Every other day, starting from day 0 to day 14 of differentiation, cells (n=4 cultures per time point and experimental group) were lysed in TriPure. After RNA extraction, cDNA synthesis was performed using M-MLV reverse transcriptase (Promega Benelux, Leiden, the Netherlands; catalogue number: M1705), random primers, dNTPs and RNasin ribonuclease inhibitor (all from Promega Benelux) and 1 µg of input RNA. Real-time PCR was carried out on a CFX96 PCR machine (Bio-Rad Laboratories, Veenendaal, the Netherlands) using GoTaq qPCR master mix (Promega Benelux; catalogue number: A6002). mRNA expression was normalized to that of the ribosomal protein-encoding housekeeping gene *Rplp0*, also known as *36b4*. Data was expressed as means ± standard error of the mean (SEM) of arbitrary units determined using the $2^{-\Delta CT}$ method. The intron-spanning primer pairs used are listed in Table 1.

Table 1 – List of primer sequences for RT-qPCR

Gene	Forward primer	Reverse primer
Rplp0	GGACCCGAGAAGACCTCCTT	GCACATCACTCAGAATTTCAATGG
Fabp4	ACACCGAGATTTCCTTCAAACTG	CCATCTAGGGTTATGATGCTCTTCA
Lpl	CCCTAAGGACCCCTGAAGAC	GGCCCGATACAACCAGTCTA
Ppargc1a	TGCTAGCGGTTCTCACAGAG	AGTGCTAAGACCGCTGCATT
Pparg	GTGCCAGTTTCGATCCGTAGA	GGCCAGCATCGTGTAGATGA
Prdm16	ACTTTGGATGGGAGCAGATG	CTCCAGGCTCGATGTCCTTA
Ucp1	TCAGGATTGGCCTCTACGAC	TGCATTCTGACCTTCACGAC

Statistical analysis

Data are represented as mean ± SEM. Effect of adrenergic stimuli on BPAs was analysed by two-way ANOVA with Dunnet's *post hoc* test. GraphPad Prism version 6.0 (GraphPad Software, La Jolla, CA) was used for all calculations. Differences at P values < 0.05 were considered statistically significant.

Results

Generation of iBPAs

Since primary BPAs gradually become senescent and stop proliferating at about PD18 (*Figure 1B*), the cells were transduced with an LV conferring dox-dependent expression of the betapolyomavirus oncoprotein LT (*Figure 1A*) and kept in dox-containing culture medium. In contrast to untransduced control cells (nBPAs) , the LT-expressing BPAs kept proliferating at the same speed for at least 60 PDs without showing any conspicuous signs of senescence (*Figure 1B*). To directly compare their proliferation rate and morphology, equal numbers of nBPAs and transduced BPAs (tBPAs) from PD18 were plated at a cell density corresponding to a confluency of 20% and cultured in medium without (nBPAs, tBPAs) or with (tBPAs) dox. Four days later microscopic images were taken. Whereas the cell density of the nBPAs remained

constant, the confluency of the dox-treated tBPA cultures increased to approximately 40 and 90% in the absence and presence of dox, respectively (*Figure 1C*). Moreover, after transduction, the cells maintained a fibroblast-like morphology (*Figure 1C*). Western blot analysis and immunofluorescence microscopy confirmed LT expression in tBPAs but not in nBPAs (*Figure 1D and E*). Taken together, the expression of LT enabled BPAs to continuously proliferate and bypass senescence, therefore, we named these cells immortalized BPAs (iBPAs).

iBPAs are clonogenic and possess long-term inducible expansion capacity

From over 50 rapidly growing cell clones, clone #6 was picked to further study the long-term dox-dependent proliferation capacity of iBPAs since it was one of the most adipogenic clones (see below). First, LT expression of clone #6 cells of PD40 and PD100 before (day 0) and after (day 2, 4, 6 and 8) dox removal were compared by western blotting and immunofluorescence staining. Both PD40 and PD100 cells displayed dox-inducible LT expression, *i.e.* LT was highly expressed in the presence of dox, and LT levels gradually dropped in its absence, being no longer detectable at 6 days after dox removal (*Figure 2A, B and C*). Moreover, quantitative analysis of the western blot data showed no statistically significant difference in LT levels between PD40 and PD100 iBPAs cultured in the presence, or for different days, in the absence of dox (*Figure 2B and C*). Consistently, iBPAs of PD40 and PD100 possessed very similar dox-inducible proliferation capacity as shown by immunostaining for the cellular proliferation marker Ki-67 (Supplementary Figure 1). In the presence of dox, cells proliferated with an average doubling time of 19 hours, whereas in the absence of dox, the cell number slightly increased up to day 4 and then stayed constant in both PD40 as well as PD100 iBPAs (*Figure 2D*). The small increase in the number of iBPAs during the first 4 days after dox removal, which is also evident in Fig. 1C, is likely due to the slow decline of the LT level following transgene silencing. To sum up, iBPAs maintain a high proliferation rate for at least 100 PDs.

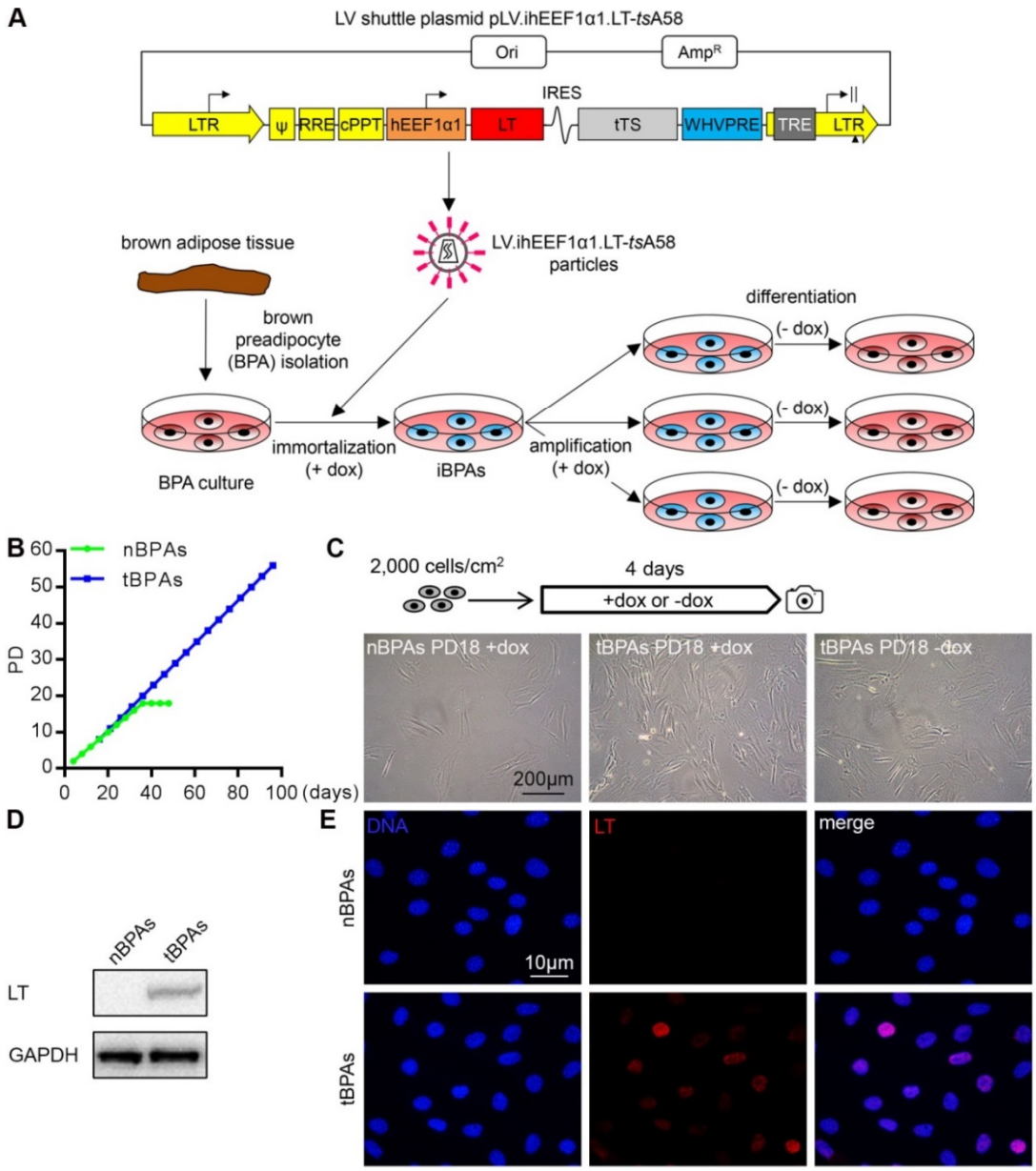

Figure 1. Conditional immortalization of BPAs

(A) Schematic representation of LV shuttle plasmid and protocol to generate conditionally immortalized BPAs. Ori, bacterial origin of replication. Amp^R, *Escherichia coli ß-lactamase* gene. LTR, human immunodeficiency virus type 1 (HIV1) long terminal repeat. Ψ, HIV1 packaging signal. RRE, HIV1 Rev-responsive element. cPPT, HIV1 central polypurine tract and termination site. hEEF1α1, human *eukaryotic translation elongation factor 1A1* gene promoter. LT, coding sequence of the temperature-sensitive mutant LT protein tsA58[34]. IRES, encephalomyocarditis virus internal ribosome entry site. tTS, coding sequence of the hybrid tetracycline-controlled transcriptional repressor TetR-KRAB[24]. WHVPRE, woodchuck hepatitis virus posttranscriptional regulatory element. TRE, tetracycline-responsive promoter element consisting of 7 repeats of a 19-nucleotide tetracycline operator (tetO) sequence. (B) Growth curves of nBPAs and tBPAs. The tBPAs continued to expand after the nBPAs had become senescent. Cells were cultured in the presence of dox. (C) Microscopic images showing the cell density and morphology at PD18 of nBPAs cultured with dox and of tBPAs cultured with or without dox. (D, E) Confirmation of LT expression in dox-exposed tBPAs (PD 18) by western blot and immunofluorescence staining. In both cases, dox-treated nBPAs of PD 18 served as negative controls.

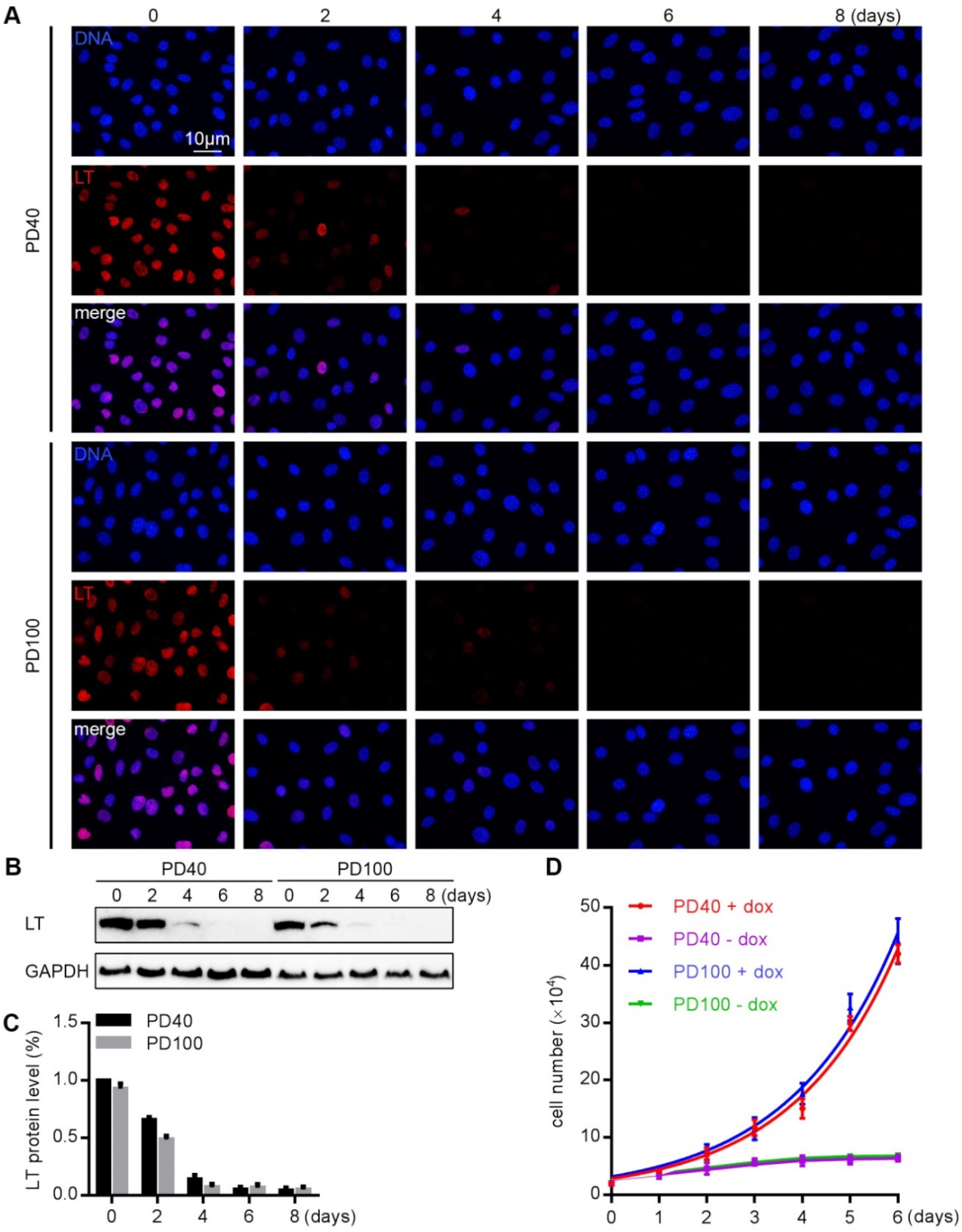

Figure 2. Dox-dependent LT expression and proliferation of iBPAs.
(A) Fluorographs of clone #6 iBPAs of PB40 and PD100 stained with the DNA binding dye Hoechst 33342 (blue) and for the SV40 LT protein (red) before (0) and at 2, 4, 6 and 8 days after dox removal. (B, C) Western blot analysis of LT expression of clone #6 iBPAs at PD40 and PD100 before (0) and at 2, 4, 6 and 8 days after dox removal. (D) Quantification of cell numbers in PD40 and PD100 cultures of clone #6 iBPAs exposed for the indicated days to medium with or without dox.

iBPAs possess adipogenic capacity

In order to assess the adipogenic capacity, cells from each clone were cultured in growth medium and when these clonal preadipocyte cell lines reached 100% confluence, dox was removed from the culture at which time point the cells were induced to differentiate to brown adipocytes under adipogenic culture conditions for 14 days (*Figure 3A*). Clone #6 and #7 cells were most adipogenic based on the extent of lipid droplet formation and *Ucp1* expression level (Supplementary Figure 2). To better characterize the adipogenic potential of these two clones, microscopic images of cell cultures subjected to adipogenic differentiation conditions were taken every two days. The cells of both clones gradually accumulated small lipid droplets acquiring the multilocular typical for brown fat cells and after 14 days of adipogenic differentiation > 90% of the cells was lipid-laden (*Figure 3B*). PD40 iBPAs were further analysed by RT-qPCR to assess the expression of brown adipocyte markers in the time course of differentiation. The unique brown fat marker *Ucp1* showed a robust induction at the RNA level starting at day 4 of adipogenic differentiation for both clones (*Figure 3C*). *Ucp1* peaked at differentiation day 12 for clone #6 and at differentiation day 10 for clone #7 (*Figure 3C*). The transcriptional coactivators PR domain containing 16 (*Prdm16, Figure 3D*) and peroxisome proliferator-activated receptor gamma coactivator 1-α (*Ppargc1a, Figure 3E*), the peroxisome proliferator-activated receptor γ (*Pparg, Figure 3F*), fatty acid binding protein 4 (*Fabp4, Figure 3G*) and lipoprotein lipase (*Lpl, Figure 3H*) followed similar patterns of expression, *i.e.* expression of all these markers was induced from the start of adipogenic differentiation and, except for *Lpl*, peaked at differentiation day 12. Based on these data, we conclude that following conditional immortalization primary murine BPAs retain their adipogenic capacity and that optimal differentiation of iBPAs is reached at 12-14 days after initiation of adipogenesis.

Extensive proliferation reduces the adipogenic capacity of iBPAs

There is no reduction in the adipogenic capacity of iBPAs at least until PD64 (data not shown). To study what would happen afterwards, clone #6 and #7 cells at PD100 were exposed to adipogenic differentiation medium and the expression patterns of the brown fat marker genes were assessed. After 100 doublings, only approximately 30% of the cells contained multiple lipid droplets at differentiation day 14 (Supplementary Figure 3) indicating incompletely preservation of adipogenic capacity. Moreover, the expression of *Ucp1* in clone #6 cells was up to 50-fold lower at PD100 than at PD40. However, exposure to adipogenic differentiation medium still resulted in an approximately 1000-fold upregulation of *Ucp1* expression at differentiation day 12 (*Figure 4A*). In contrast, clone #7 cells of PD100 showed hardly any increase in *Ucp1* expression following adipogenic stimulation (*Figure 4A*). Both clone #6 and #7 cells showed a clear increase in the expression of the other brown fat marker genes after exposure to adipogenic differentiation conditions (*Figure 4B-F*). However, for all these gene, expression was lower at PD100 than at PD40, except for *Lpl*, which was higher expressed at PD100 (*Figure 4G*). Moreover, the expression of these genes did not peak at day 12 of differentiation as observed at PD40, but earlier. In conclusion, late passage iBPAs differentiate less well into brown adipocytes than early passage iBPAs based on lipid droplet formation and brown fat marker gene expression.

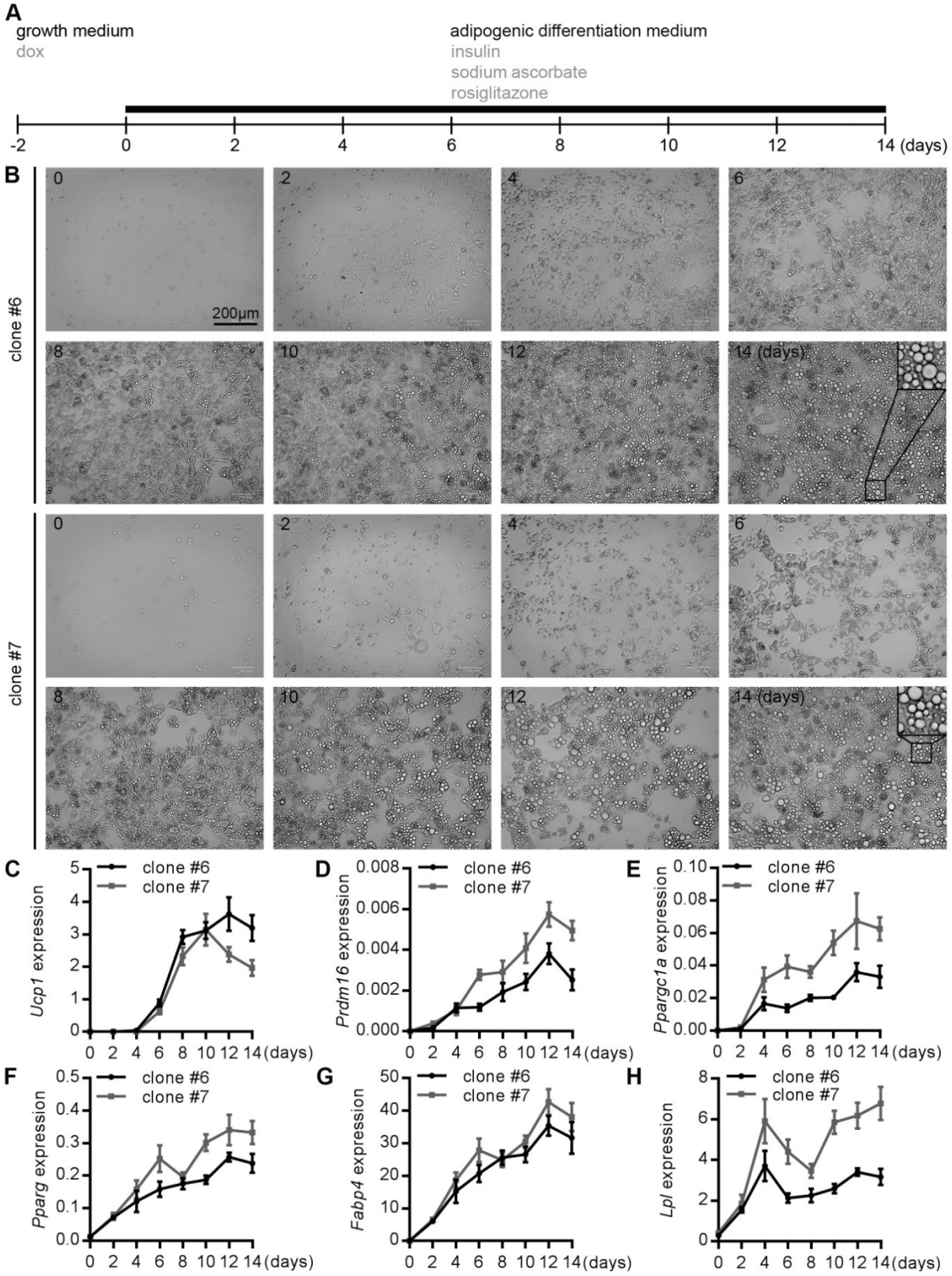

Figure 3. Comparison of the adipogenic potential of 2 different iBPA clones. (A) Protocol used to differentiate iBPAs towards brown adipocytes. (B) Phase contrast images showing the morphological changes associated with the adipogenic differentiation of clone #6 and #7 iBPAs of PD40. (C) RT-qPCR analysis of *Ucp1*, *Prdm16*, *Ppargc1a*, *Pparg*, *Fabp4* and *Lpl* gene expression in clone #6 and #7 iBPAs at PD40 on the indicated days of adipogenic differentiation normalized to *Rplp0* expression. Data are presented as means ± SEM (n=4).

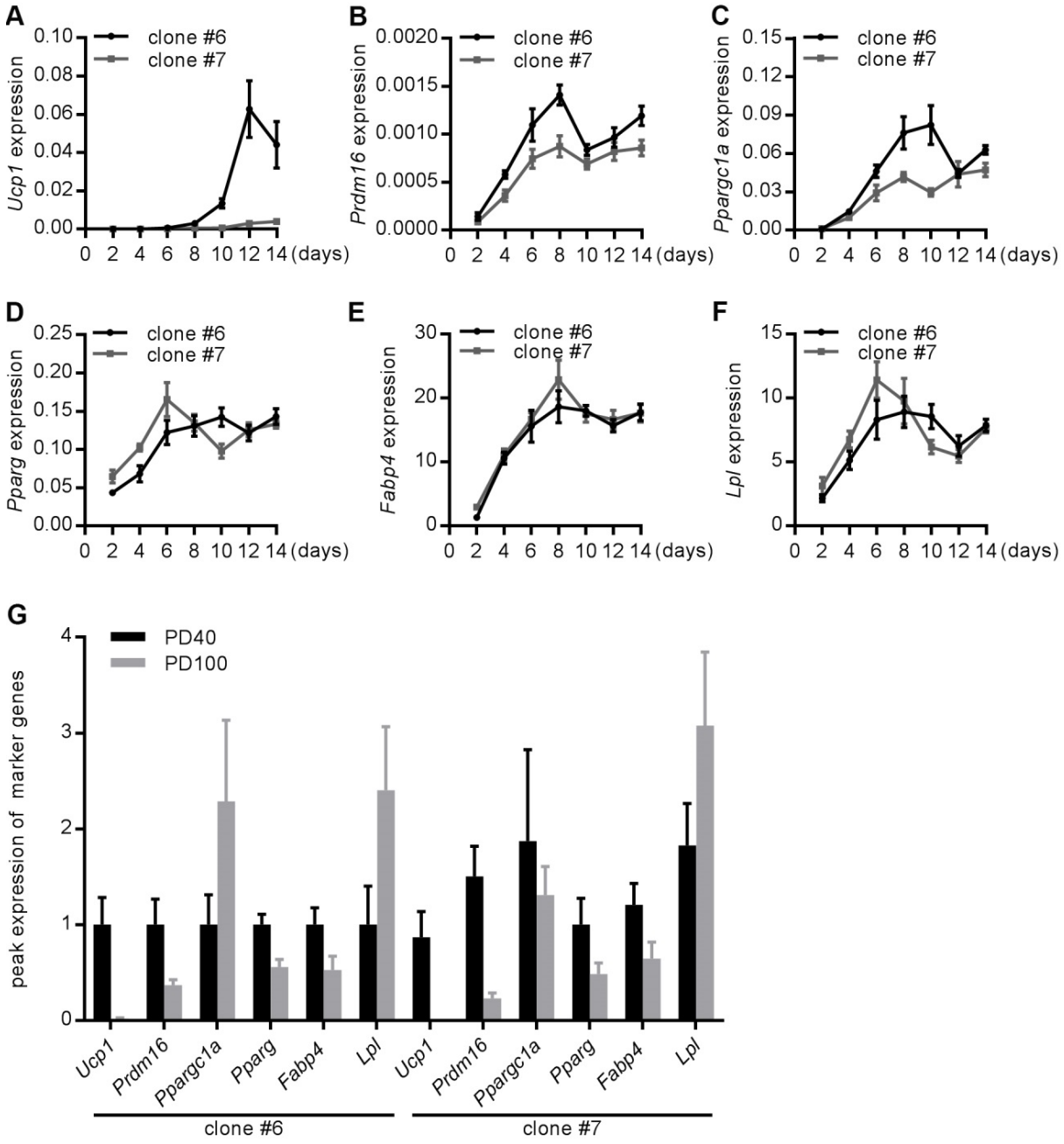

Figure 4. Adipogenic potential of massively amplified iBPA clones.
(A-F) RT-qPCR analysis of *Ucp1, Prdm16, Ppargc1a, Pparg, Fabp4* and *Lpl* gene expression in clone #6 and #7 iBPAs at PD100 on the indicated days of adipogenic differentiation normalized to *Rplp0* expression. (G) Peak expression of the selected marker genes in clone #6 and #7 iBPAs at PD40 and PD100 during adipogenic differentiation. Gene expression levels are expressed relative to those of clone #6 at PD40, which were set at 1. Data are presented as means ± SEM (n=4).

β3-adrenoceptor agonists stimulate lipolysis in adipogenically differentiated iBPAs

To investigate the response of adipogenically differentiated iBPAs to adrenergic stimulation, the cells were stimulated with the general adrenergic agonist NA[28] or with the specific β3 adrenoceptor agonist CL316243[29,30]and glycerol release was quantified. The glycerol concentration in the culture medium was significantly increased upon 8 hours of stimulation with NA (+1659%, $P < 0.001$ for clone #6, +2028%, $P < 0.001$ for clone #7) and CL316243 (+1647%, $P < 0.001$ for clone #6, +1598%, $P < 0.001$ for clone #7) pointing to increased intracellular lipolysis (*Figure 5A*). Furthermore, *Ucp1* expression was determined after 8 hours of NA and CL316243 incubation. Consistent with the increased lipolysis, *Ucp1* expression was significantly increased after NA (+231%, $P < 0.001$ for clone #6, +121%, $P < 0.05$ for clone #7) or CL316243 (+155%, $P < 0.01$ for clone #6, +181%, $P < 0.01$ for clone #7) stimulation in both clones (*Figure 5B*). Together, these data demonstrate that the iBPAs are responsive to β3-adrenergic stimulation.

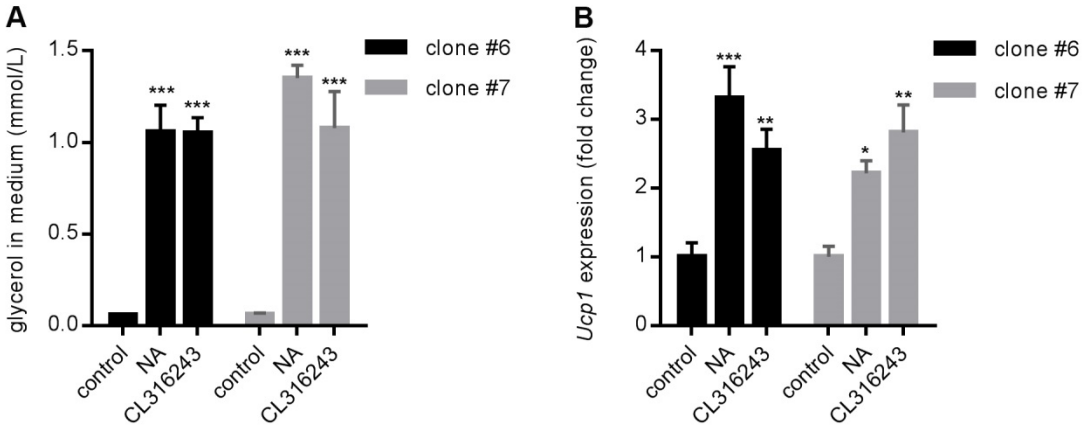

Figure 5. Effect of adrenergic stimulation on *Ucp1* expression and lipolysis of adipogenically differentiated iBPAs. (A, B) Clone #6 and #7 iBPAs of PD46 at differentiation day 12 were stimulated with 1 μM NA or 10 μM CL316243 for 8 hour after which glycerol release in the supernatant (A), and *Ucp1* RNA levels (B) were measured. Data are means ± SEM (n=4).

Discussion

Monoclonal lines of BPAs with inducible proliferation ability

Permanent immortalization of BPAs has been proven to be an effective tool to study brown adipocyte biology and responses to pharmacological treatments[14-18]. However, the rapid loss of robust adipogenic capacity during cell amplification and the potential effects of exogenous expression of immortalization genes such as LT on BPAs remain unresolved issues using this approach. In this study, we developed a system enabling the robust and tightly controlled expansion of monoclonal populations of BPAs by endowing the cells with a dox-regulated SV40 LT expression module. The presence of dox in the culture medium induced LT expression and caused rapid iBPA expansion, while removing dox released the proliferation pressure and prepared the cells for subsequent adipogenic differentiation. Our monoclonal iBPA lines allow synchronous adipogenic differentiation of BPAs, providing a clear advantage in the assessment of differentiation stage-dependent gene expression profiles and epigenetic changes. Moreover, the use, in previous studies, of permanent immortalization gene expression to generate BPA lines poses a problem to their application in transplantation experiments, whereas the tightly controlled LT expression system used in this study created an opportunity for this iBPAs to become a transplantable cell source. Also, recent studies have shown that mature brown adipocytes retain proliferative capacity[28,29], although the mechanism(s) involved is/are largely unknown. It will hence be of interest to investigate what happens when adipogenically differentiated iBPAs are re-exposed to dox. If this would cause them to start dividing again, it might (i) provide a good model system to gain more insight into the pathways involved in BAT hyperplasia and (ii) allow dox-dependent regulation of the size of the brown fat compartment *in vivo*.

LT expression in adipocyte differentiation

Mature lipid-filled adipocytes are post-mitotic, requiring BPAs to exit the cell cycle for terminal differentiation. This may limit the differentiation potential of BPA lines with permanent immortalization gene expression. In addition, studies have shown that LT inhibits white adipogenesis but facilitates brown adipogenesis by inactivation of the pRB pathway[20,30,31]. A better understanding of the role of LT in adipogenesis will help to further understand the mechanisms of brown adipogenesis as well as the conversion of white into brown fat cells and *vice versa*. iBPAs are unique in their ability to vary the timing of LT expression and therefore pocket protein activity in relation to the moment of adipogenic stimulation. This property makes iBPAs particularly attractive for studying the role of cell cycle regulators including those directly targeted by LT in BPA differentiation.

Long-term differentiation capacity of iBPAs

iPBAs retained full adipogenic capacity for at least 64 PDs, implying that $> 10^{19}$ brown adipocytes could be generated from a single preadipocyte. This provides an abundant cell source for cell-based disease modelling and raises the possibility to endow mice with extra brown fat tissue via cell transplantation. This brown fat tissue could be provided with new properties by *ex vivo* genetic engineering thereby creating

additional opportunities for fundamental and applied research. Beyond 64 PDs, the cells show a less pronounced differentiated brown adipocyte phenotype based on the reduced expression of *Ucp1* and other brown fat markers at PD100 in comparison to PD40. The reason could be that proliferation of iBPAs causes gradual loss of the epigenetic modifications required for maintaining their cell type-specific memory[32,33], resulting in a progressive decrease in adipogenic capacity upon repeated passaging.

Difference in adipogenic capacity between diffent iBPA clones

As shown in Supplementary Figure 2, different iBPA clones differ in their ability to differentiate into brown fat cells. The reason for this is unclear but it may have to do with (i) some (intrinsic) heterogeneity of the starting material and/or (ii) the number and location of the chromosomally integrated transgenes. A comparison of the transcriptional signatures of iBPAs from a single source but with different adipogenic capacity may be help to broaden the understanding of the molecular pathways orchestrating brown fat formation.

Conclusion

In this study, we established lines of conditionally immortalized murine brown preadipocytes with long-term proliferation ability (at least 100 PDs) and adipogenic capacity (at least 64 PDs). Following adipogenesis , these cells displayed a multilocular appearance, gene expression signature and metabolic capacity alike brown adipocytes. The generated cell lines could have many applications and, for example, be used to investigate BPA proliferation and differentiation, brown (pre)adipocyte metabolism and regulation of *Ucp1* activity and thermogenesis, for brown (pre)adipocyte-based disease modelling and for BPA transplantation studies.

References

1. Cypess AM, Lehman S, Williams G, Tal I, Rodman D, Goldfine AB, Kuo FC, Palmer EL, Tseng YH, Doria A, Kolodny GM, Kahn CR. Identification and importance of brown adipose tissue in adult humans. *N Engl J Med* 2009;**360**:1509-1517.
2. Tseng YH, Cypess AM, Kahn CR. Cellular bioenergetics as a target for obesity therapy. *Nat Rev Drug Discov* 2010;**9**:465-482.
3. Bauer-Kreisel P, Goepferich A, Blunk T. Cell-delivery therapeutics for adipose tissue regeneration. *Adv Drug Deliv Rev* 2010;**62**:798-813.
4. Townsend K, Tseng YH. Brown adipose tissue: Recent insights into development, metabolic function and therapeutic potential. *Adipocyte* 2012;**1**:13-24.
5. Tang W, Zeve D, Suh JM, Bosnakovski D, Kyba M, Hammer RE, Tallquist MD, Graff JM. White fat progenitor cells reside in the adipose vasculature. *Science* 2008;**322**:583-586.
6. Rodeheffer MS, Birsoy K, Friedman JM. Identification of white adipocyte progenitor cells in vivo. *Cell* 2008;**135**:240-249.
7. Zhang H, Schulz TJ, Espinoza DO, Huang TL, Emanuelli B, Kristiansen K, Tseng YH. Cross talk between insulin and bone morphogenetic protein signaling systems in brown adipogenesis. *Mol Cell Biol* 2010;**30**:4224-4233.
8. Kajimura S, Seale P, Kubota K, Lunsford E, Frangioni JV, Gygi SP, Spiegelman BM. Initiation of myoblast to brown fat switch by a PRDM16-C/EBP-beta transcriptional complex. *Nature* 2009;**460**:1154-1158.
9. Cannon B, Nedergaard J. Developmental biology: Neither fat nor flesh. *Nature* 2008;**454**:947-948.
10. Seale P, Bjork B, Yang W, Kajimura S, Chin S, Kuang S, Scime A, Devarakonda S, Conroe HM, Erdjument-Bromage H, Tempst P, Rudnicki MA, Beier DR, Spiegelman BM. PRDM16 controls a brown fat/skeletal muscle switch. *Nature* 2008;**454**:961-967.
11. Schulz TJ, Tseng YH. Brown adipose tissue: development, metabolism and beyond. *Biochem J* 2013;**453**:167-178.
12. Stanford KI, Goodyear LJ. The therapeutic potential of brown adipose tissue. *Hepatobiliary Surg Nutr* 2013;**2**:286-287.
13. Cohen P, Levy JD, Zhang Y, Frontini A, Kolodin DP, Svensson KJ, Lo JC, Zeng X, Ye L, Khandekar MJ, Wu J, Gunawardana SC, Banks AS, Camporez JP, Jurczak MJ, Kajimura S, Piston DW, Mathis D, Cinti S, Shulman GI, Seale P, Spiegelman BM. Ablation of PRDM16 and beige adipose causes metabolic dysfunction and a subcutaneous to visceral fat switch. *Cell* 2014;**156**:304-316.
14. Forest C, Doglio A, Ricquier D, Ailhaud G. A preadipocyte clonal line from mouse brown adipose tissue. Short- and long-term responses to insulin and beta-adrenergics. *Exp Cell Res* 1987;**168**:218-232.
15. Irie Y, Asano A, Canas X, Nikami H, Aizawa S, Saito M. Immortal brown adipocytes from p53-knockout mice: differentiation and expression of uncoupling proteins. *Biochem Biophys Res Commun* 1999;**255**:221-225.
16. Klaus S, Choy L, Champigny O, Cassard-Doulcier AM, Ross S, Spiegelman B,

Ricquier D. Characterization of the novel brown adipocyte cell line HIB 1B. Adrenergic pathways involved in regulation of uncoupling protein gene expression. *J Cell Sci* 1994;**107 (Pt 1)**:313-319.
17. Kozak UC, Held W, Kreutter D, Kozak LP. Adrenergic regulation of the mitochondrial uncoupling protein gene in brown fat tumor cells. *Mol Endocrinol* 1992;**6**:763-772.
18. Zennaro MC, Le Menuet D, Viengchareun S, Walker F, Ricquier D, Lombes M. Hibernoma development in transgenic mice identifies brown adipose tissue as a novel target of aldosterone action. *J Clin Invest* 1998;**101**:1254-1260.
19. Forest C, Doglio A, Casteilla L, Ricquier D, Ailhaud G. Expression of the mitochondrial uncoupling protein in brown adipocytes. Absence in brown preadipocytes and BFC-1 cells. Modulation by isoproterenol in adipocytes. *Exp Cell Res* 1987;**168**:233-246.
20. Hansen JB, Jørgensen C, Petersen RK, Hallenborg P, De Matteis R, Bøye HA, Petrovic N, Enerbäck S, Nedergaard J, Cinti S. Retinoblastoma protein functions as a molecular switch determining white versus brown adipocyte differentiation. *Proceedings of the National Academy of Sciences* 2004;**101**:4112-4117.
21. Molchadsky A, Ezra O, Amendola PG, Krantz D, Kogan-Sakin I, Buganim Y, Rivlin N, Goldfinger N, Folgiero V, Falcioni R, Sarig R, Rotter V. p53 is required for brown adipogenic differentiation and has a protective role against diet-induced obesity. *Cell Death Differ* 2013;**20**:774-783.
22. Szulc J, Wiznerowicz M, Sauvain MO, Trono D, Aebischer P. A versatile tool for conditional gene expression and knockdown. *Nat Methods* 2006;**3**:109-116.
23. Liu J, Volkers L, Jangsangthong W, Bart CI, Engels MC, Zhou G, Schalij MJ, Ypey DL, Pijnappels DA, de Vries AAF. Generation and primary characterization of iAM-1, a versatile new line of conditionally immortalized atrial myocytes with preserved cardiomyogenic differentiation capacity. *Cardiovasc Res* acceptted.
24. Deuschle U, Meyer WK, Thiesen HJ. Tetracycline-reversible silencing of eukaryotic promoters. *Mol Cell Biol* 1995;**15**:1907-1914.
25. Feola I, Teplenin A, de Vries AA, Pijnappels DA. Optogenetic engineering of atrial cardiomyocytes. *Methods Mol Biol* 2016;**1408**:319-331.
26. Majumder R, Engels MC, de Vries AA, Panfilov AV, Pijnappels DA. Islands of spatially discordant APD alternans underlie arrhythmogenesis by promoting electrotonic dyssynchrony in models of fibrotic rat ventricular myocardium. *Sci Rep* 2016;**6**:24334.
27. Yu Z, Liu J, van Veldhoven JP, AP IJ, Schalij MJ, Pijnappels DA, Heitman LH, de Vries AA. Allosteric modulation of Kv11.1 (hERG) channels protects against drug-induced ventricular arrhythmias. *Circ Arrhythm Electrophysiol* 2016;**9**:e003439.
28. Okamatsu-Ogura Y, Fukano K, Tsubota A, Nio-Kobayashi J, Nakamura K, Morimatsu M, Sakaue H, Saito M, Kimura K. Cell-cycle arrest in mature adipocytes impairs BAT development but not WAT browning, and reduces adaptive thermogenesis in mice. *Scientific reports* 2017;**7**:6648.
29. Fukano K, Okamatsu-Ogura Y, Tsubota A, Nio-Kobayashi J, Kimura K. Cold

exposure induces proliferation of mature brown adipocyte in a ß3-adrenergic receptor-mediated pathway. *PloS one* 2016;**11**:e0166579.
30. Cherington V, Morgan B, Spiegelman BM, Roberts TM. Recombinant retroviruses that transduce individual polyoma tumor antigens: effects on growth and differentiation. *Proceedings of the National Academy of Sciences* 1986;**83**:4307-4311.
31. Higgins C, Chatterjee S, Cherington V. The block of adipocyte differentiation by a C-terminally truncated, but not by full-length, simian virus 40 large tumor antigen is dependent on an intact retinoblastoma susceptibility protein family binding domain. *J Virol* 1996;**70**:745-752.
32. Avgustinova A, Benitah SA. Epigenetic control of adult stem cell function. *Nature Reviews Molecular Cell Biology* 2016.
33. Wagner W. Implications of long-term culture for mesenchymal stem cells: genetic defects or epigenetic regulation? *Stem Cell Res Ther* 2012;**3**:54.
34. Loeber G, Tevethia MJ, Schwedes JF, Tegtmeyer P. Temperature-sensitive mutants identify crucial structural regions of simian virus 40 large T antigen. *J Virol* 1989;**63**:4426-4430.

Supporting information

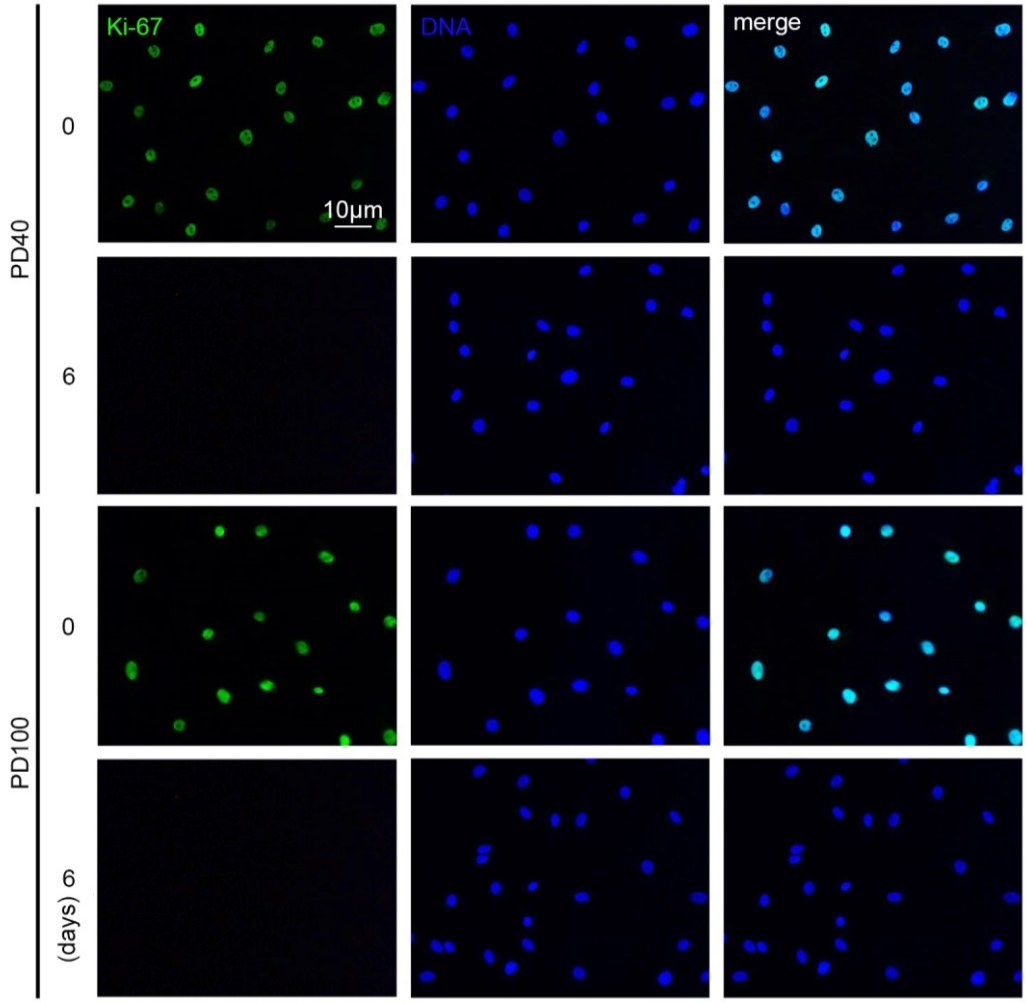

Supplementary Figure 1. Fluorescence images of iBPAs maintained in growth medium before (0) and at 6 days after dox removal immunostained for the proliferation marker Ki-67 (green). Nuclei are visualized with Hoechst 33342 (blue).

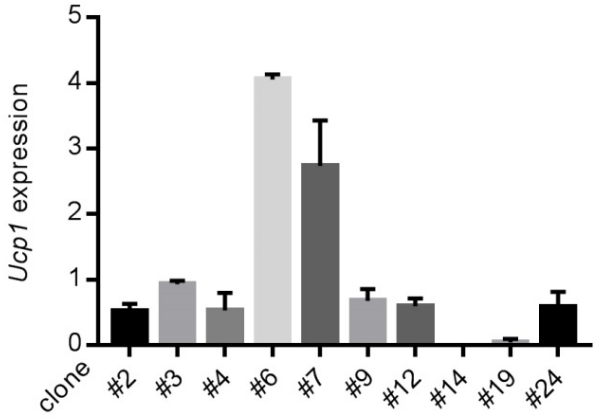

Supplementary Figure 2. RT-qPCR analysis of *Ucp1* expression in 10 different iBPA clones on differentiation day 12 normalized to *Rplp0* expression. Data are presented as means ± SEM (n=4).

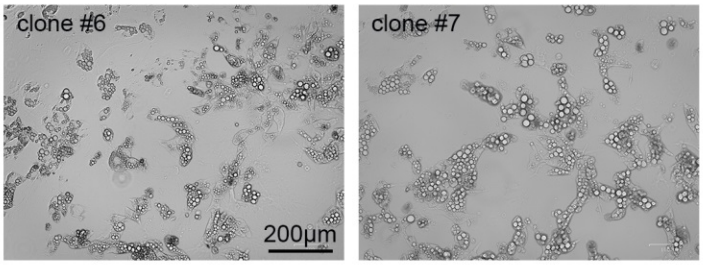

Supplementary Figure 3. Light microscopic images showed the morphology of clone #6 and #7 iBPAs at PD100 on differentiation day 12.